

Ionic conductivity studies of $\text{La}_{0.55}\text{Li}_{0.40}\text{ZrO}_{3-\delta}$ and Zr doped $\text{La}_{0.55}\text{Li}_{0.40}\text{TiO}_{3-\delta}$

B SINGH†, S NISHAD and S SIDDIQUI

Materials Chemistry Laboratory, Centre of Material Sciences, University of Allahabad, Prayagraj – 211002, India

†Author for correspondence (brajendr@gmail.com; brajendr@allduniv.ac.in)

Received: 20.11.2019 ; Revised : 10.12.2019 ; Accepted : 7.1.2020

Abstract. We report the synthesis and conductivity properties of $\text{La}_{0.55}\text{Li}_{0.40}\text{ZrO}_{3-\delta}$ and Zr doped $\text{La}_{0.55}\text{Li}_{0.40}\text{Ti}_{0.9}\text{Zr}_{0.1}\text{O}_{3-\delta}$ perovskite oxide. X-ray diffraction (XRD) pattern shows the orthorhombic perovskite structure for $\text{La}_{0.55}\text{Li}_{0.40}\text{ZrO}_{3-\delta}$ and $\text{La}_{0.55}\text{Li}_{0.40}\text{Ti}_{0.9}\text{Zr}_{0.1}\text{O}_{3-\delta}$. Conductivity has been found increased with the increase in temperature and frequency in both the compositions. $\text{La}_{0.55}\text{Li}_{0.40}\text{ZrO}_{3-\delta}$ shows 1.04×10^{-2} S/cm conductivity at room temperature (25°C) which increases upto maximum 5.1×10^{-2} S/cm for 300°C. $\text{La}_{0.55}\text{Li}_{0.40}\text{TiO}_{3-\delta}$ shows maximum conductivity 2.5×10^{-3} S/cm at room temperature (25°C). $\text{La}_{0.55}\text{Li}_{0.40}\text{Ti}_{0.9}\text{Zr}_{0.1}\text{O}_{3-\delta}$ shows maximum conductivity 7.21×10^{-3} S/cm at room temperature. This is the first report of synthesis of single phase of $\text{La}_{0.55}\text{Li}_{0.40}\text{ZrO}_{3-\delta}$ oxide and this material shows high conductivity from room temperature to temperature 450 °C.

Keywords: Ceramics, Conductivity; High temperature synthesis; Impedance; Cole-Cole plots

PACS: 66.30.Dn; 82.45.Xy; 81.20.Ev; 84.37.+q

1. Introduction

Rechargeable batteries have become an integral part of modern electronic devices. Li ion rechargeable batteries have significant advantages of better cycle life, low self discharge, high energy density and low weight [1-6]. These batteries use a liquid electrolyte which makes these batteries venerable for shocks and miniaturization. To overcome these effects, solid electrolytes have been envisaged as an alternative to liquid electrolytes. Several types of lithium solid electrolytes have been reported, including perovskite-type titanates [1], garnet-type zirconets [2], NASICON-type phosphates [3] and

LISICON-type sulfides [4], which show Li ion conductivity. Latie and Belous et al. have reported the first lithium ion conducting perovskite by hetero-valent substitution of La^{3+} by Li^+ cations in the A-site deficient perovskite $\text{La}_{2/3}\text{TiO}_3$ [5-6]. Perovskite [ABO_3] oxides have been extensively studied due to its novel electronic, magnetic, magnetoelectric and ion conducting properties [7-9]. Perovskite properties can be tuned by chemical substitution at A, or B site or making vacancy at A or B or O site [10,11]. The crystal structure and physical properties of perovskites are also very sensitive to calcination and sintering temperatures, quenching, heating and cooling rates, sintering timing, sintering in oxidation/reduction/ambient atmospheres[11]. It is essential to reveal the relationship of structural stability of electrolytes with the ionic conduction during material design for better performance of lithium batteries [12]. It has been shown by Harada et al. that the perovskites having compositions $\text{La}_{2/3-x}\text{Li}_{3x}\text{TiO}_3$ ($0.03 < x < 0.167$) remain stable in spite of A site deficiency [13]. These perovskites crystallizes with various crystal symmetries depending on the composition and synthesis methods. $\text{La}_{0.67-x}\text{Li}_{3x}\text{TiO}_3$ ($x=0.11$) crystallizes in cubic with space group $Pm3m$ [13], $\text{Li}_{0.5}\text{La}_{0.5}\text{TiO}_3$ crystallizes in hexagonal with space group $R3c$ [14] and tetragonal with space group $P4/mmm$ is formed with an ordered distribution of La ions on the perovskite A-sites along the c-axis in $\text{La}_{2/3-x}\text{Li}_{3x}\text{TiO}_3$ ($0.08 < x < 0.16$)[15]. Orthorhombic ($Cmmm$) structure with lower lithium content is formed in $\text{La}_{2/3-x}\text{Li}_{3x}\text{TiO}_3$ ($x < 0.06$)[16-17]. $\text{La}_{2/3-x}\text{Li}_{3x}\text{TiO}_3$ has stimulated a wide interest because of its high bulk Li ion conductivity $\sim 10^{-3}$ S/cm. High Li ion conductivity in $\text{La}_{2/3-x}\text{Li}_{3x}\text{TiO}_3$ can be attributed to the presence of many equivalent sites which enable the lithium ions to move freely along A-site vacancies which is affected by the degree of order on the A-site and the charge carrier concentration [18]. Uhlmann et al. have shown the working of Lithium Lanthanum Titanate as solid electrolyte in Lithium-air batteries [19]. Hang at al. have shown the use of aluminium doped Lithium Lanthanum Titanate as solid electrolyte in aqueous rechargeable lithium – metal based batteries [20]. Bhuvanesh et al. have suggested the use of d^0 cations such as Ti^{4+} , Zr^{4+} and Ta^{5+} for B cations in lithium ion conducting perovskite-type oxides to distort BO_6 Octahedra from six equal B-O bonds to short and long B-O bonds in perovskite oxides to increase the Li ion conductivity [21]. Among solid electrolyte materials, garnet-type $\text{La}_3\text{Li}_7\text{Zr}_2\text{O}_{12}$ is one of the most promising candidates due to its relatively high ionic

conductivity and chemical stability in contact with Li metal [22-23]. It has been shown in literature that high-temperature synthesized $\text{Li}_7\text{La}_3\text{Zr}_2\text{O}_{12}$ show conductivity $\sim 10^{-4}$ S/cm while low-temperature synthesized $\text{Li}_7\text{La}_3\text{Zr}_2\text{O}_{12}$ show conductivity $\sim 10^{-6}$ S/cm) [24]. Zr based perovskite materials might be a good option as (i) Zr has bigger size than Ti so it can provide stable structure and (ii) these can show better Li ion conduction along A-site vacancies. Jena et al. could not prepare $\text{La}_{0.5}\text{Li}_{0.5}\text{ZrO}_3$ by wet chemical methods due to formation of $\text{La}_2\text{Zr}_2\text{O}_7$ and ZrO_2 phases [25]. In this manuscript, we have reported the synthesis of A site deficient $\text{La}_{0.55}\text{Li}_{0.40}\text{TiO}_{3-\delta}$, $\text{La}_{0.55}\text{Li}_{0.40}\text{Ti}_{0.9}\text{Zr}_{0.1}\text{O}_{3-\delta}$ and $\text{La}_{0.55}\text{Li}_{0.40}\text{ZrO}_{3-\delta}$ perovskite oxides. We have explored the temperature and frequency dependent conductivity properties of these materials at room temperature and higher temperatures.

2. Experimental

We had synthesized polycrystalline $\text{La}_{0.55}\text{Li}_{0.40}\text{TiO}_{3-\delta}$, $\text{La}_{0.55}\text{Li}_{0.40}\text{Ti}_{0.9}\text{Zr}_{0.1}\text{O}_{3-\delta}$ and $\text{La}_{0.55}\text{Li}_{0.40}\text{ZrO}_{3-\delta}$ samples using Lanthanum Oxide (La_2O_3), Lithium Hydroxide ($\text{LiOH} \cdot \text{H}_2\text{O}$), Titanium Oxide [TiO_2] and Zirconia Oxide (ZrO_2) precursors. Samples were prepared by solid-state method of synthesis. After weighing stoichiometric amounts, precursors were mixed in an agate mortar and grinded for 45 minutes. Grinded powder were again regrinded in 25 ml ethanol for 15 minutes for proper mixing. This grinded powder were calcined at 1200°C for 12 hours with heating and cooling rate 5° per minute. After calcination, powder were grounded and pressed it for making 10 mm diameter pellets. These pellets were sintered at 1300°C for 12 h with keeping heating and cooling rate 5° per minute. Powder X-ray diffraction method was used to examine the crystal structure of polycrystalline samples $\text{La}_{0.55}\text{Li}_{0.40}\text{TiO}_{3-\delta}$, $\text{La}_{0.55}\text{Li}_{0.40}\text{Ti}_{0.9}\text{Zr}_{0.1}\text{O}_{3-\delta}$ and $\text{La}_{0.55}\text{Li}_{0.40}\text{ZrO}_{3-\delta}$ with $\text{CuK}_{\alpha 1}$ radiation ($\lambda = 1.5405 \text{ \AA}$) at 40kV and 30 mA over 10 to 90 degree with data separation 0.02 degree. Novacontrol make Impedance analyzer (Alpha-A high performance frequency analyzer) was used to determine impedance and conductivity in the frequency range from 1Hz to 40 MHz in ambient atmosphere from room temperature 25°C to 450°C . To avoid fluctuations in data, we had pasted silver paste on the both side of sample pellets and measurements were recorded by two probe method using silver electrode.

3. Results and Discussion

Figure 1 shows the X-ray diffraction (XRD) pattern of $\text{La}_{0.55}\text{Li}_{0.40}\text{TiO}_{3-\delta}$, $\text{La}_{0.55}\text{Li}_{0.40}\text{Ti}_{0.9}\text{Zr}_{0.1}\text{O}_{3-\delta}$ and $\text{La}_{0.55}\text{Li}_{0.40}\text{ZrO}_{3-\delta}$ samples. XRD patterns of polycrystalline samples show the crystallization of $\text{La}_{0.55}\text{Li}_{0.40}\text{TiO}_{3-\delta}$ and $\text{La}_{0.55}\text{Li}_{0.40}\text{ZrO}_{3-\delta}$ in orthorhombic crystal structures.

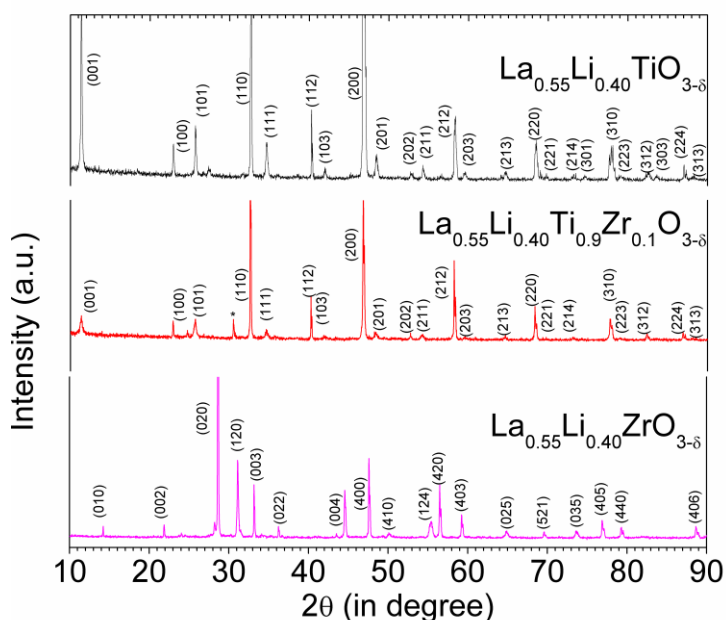


Fig. 1. X-ray diffraction patterns of polycrystalline $\text{La}_{0.55}\text{Li}_{0.40}\text{ZrO}_{3-\delta}$ perovskite oxide

As Zr substituted at Ti position in $\text{La}_{0.55}\text{Li}_{0.40}\text{TiO}_{3-\delta}$, due to bigger size of Zr, the lattice rearrangement occurs in $\text{La}_{0.55}\text{Li}_{0.40}\text{Ti}_{0.9}\text{Zr}_{0.1}\text{O}_{3-\delta}$. New peak originates ~ 30 degree in the XRD pattern of $\text{La}_{0.55}\text{Li}_{0.40}\text{Ti}_{0.9}\text{Zr}_{0.1}\text{O}_{3-\delta}$ and majority of peaks at higher angles show doublet. This behavior has been found in all three compositions. It shows the oxygen deficiency in the lattice as observed in other known perovskite oxide $\text{CaMnO}_{3-\delta}$ [11]. $\text{La}_{0.55}\text{Li}_{0.40}\text{ZrO}_{3-\delta}$ crystallizes in orthorhombic crystal system as observed by belous et al [26]. Lattice constants has been found $a = 7.6312 \text{ \AA}$, $b = 6.2308 \text{ \AA}$ and $c = 8.0898 \text{ \AA}$ for $\text{La}_{0.55}\text{Li}_{0.40}\text{ZrO}_{3-\delta}$. Tolerance factor $[t=(r_A+r_O)/\sqrt{2} (r_B+r_O)]$ has been calculated 0.8445 for $\text{La}_{0.55}\text{Li}_{0.40}\text{ZrO}_{3-\delta}$.

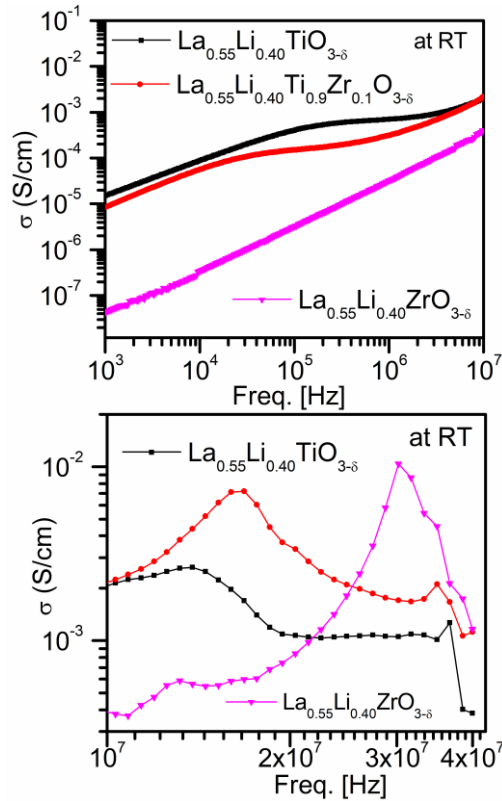


Fig. 2. Conductivity plots of sintered pellets of $\text{La}_{0.55}\text{Li}_{0.40}\text{TiO}_{3-\delta}$, $\text{La}_{0.55}\text{Li}_{0.40}\text{Ti}_{0.9}\text{Zr}_{0.1}\text{O}_{3-\delta}$ and $\text{La}_{0.55}\text{Li}_{0.40}\text{ZrO}_{3-\delta}$ recorded at room temperature (25°C).

Figure 2 shows the conductivity of $\text{La}_{0.55}\text{Li}_{0.40}\text{TiO}_{3-\delta}$, $\text{La}_{0.55}\text{Li}_{0.40}\text{Ti}_{0.9}\text{Zr}_{0.1}\text{O}_{3-\delta}$ and $\text{La}_{0.55}\text{Li}_{0.40}\text{ZrO}_{3-\delta}$ at room temperature (25°C). Maximum conductivity value has found 2.5×10^{-3} S/cm at 13MHz. At frequency 1MHz, the conductivity value is found 3.15×10^{-5} S/cm for $\text{La}_{0.55}\text{Li}_{0.40}\text{TiO}_{3-\delta}$. Maximum conductivity value has been found 1.04×10^{-2} S/cm at 30MHz and 4.15×10^{-4} S/cm at 1MHz for $\text{La}_{0.55}\text{Li}_{0.40}\text{ZrO}_{3-\delta}$. Conductivity value of $\text{La}_{0.55}\text{Li}_{0.40}\text{ZrO}_{3-\delta}$ has been found greater in comparison to the conductivity of $\text{La}_{0.55}\text{Li}_{0.40}\text{TiO}_{3-\delta}$ at room temperature in frequencies greater than 20MHz. The plotted conductivity represents the sum of the grain boundary and bulk conductivity. Figure 3 shows the conductivity of $\text{La}_{0.55}\text{Li}_{0.40}\text{TiO}_{3-\delta}$, $\text{La}_{0.55}\text{Li}_{0.40}\text{Ti}_{0.9}\text{Zr}_{0.1}\text{O}_{3-\delta}$ and $\text{La}_{0.55}\text{Li}_{0.40}\text{ZrO}_{3-\delta}$ at 100°C ,

200°C and 300°C in frequency from 1kHz to 40MHz. $\text{La}_{0.55}\text{Li}_{0.40}\text{ZrO}_{3-\delta}$ shows higher conductivities than the conductivities of $\text{La}_{0.55}\text{Li}_{0.40}\text{TiO}_{3-\delta}$, $\text{La}_{0.55}\text{Li}_{0.40}\text{Ti}_{0.9}\text{Zr}_{0.1}\text{O}_{3-\delta}$ in presence of frequencies greater than 20 MHz. Maximum conductivity attained by respective samples at specific temperature has been tabulated in table 1. At 450°C, maximum conductivity value has been found 4.1×10^{-2} S/cm at 30MHz and minimum impedance has been found 6.94 Ω at 30MHz for $\text{La}_{0.55}\text{Li}_{0.40}\text{ZrO}_{3-\delta}$.

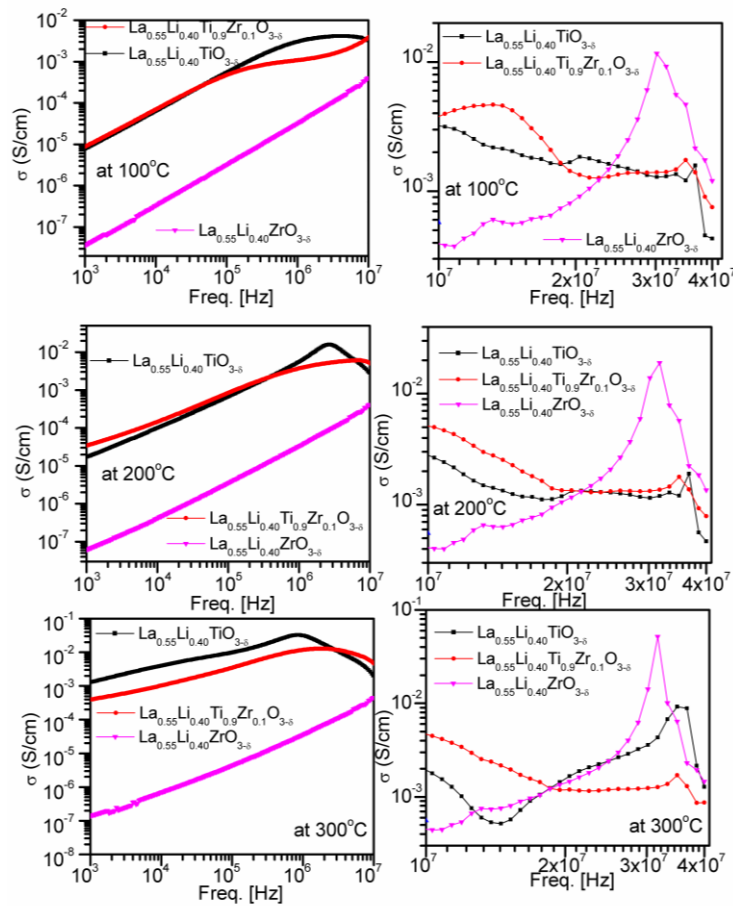


Fig. 3. Conductivity plots of sintered pellets of $\text{La}_{0.55}\text{Li}_{0.40}\text{TiO}_{3-\delta}$, $\text{La}_{0.55}\text{Li}_{0.40}\text{Ti}_{0.9}\text{Zr}_{0.1}\text{O}_{3-\delta}$ and $\text{La}_{0.55}\text{Li}_{0.40}\text{ZrO}_{3-\delta}$ recorded at 100, 200 and 300°C. The plotted conductivity represents the sum of the grain boundary and bulk conductivity.

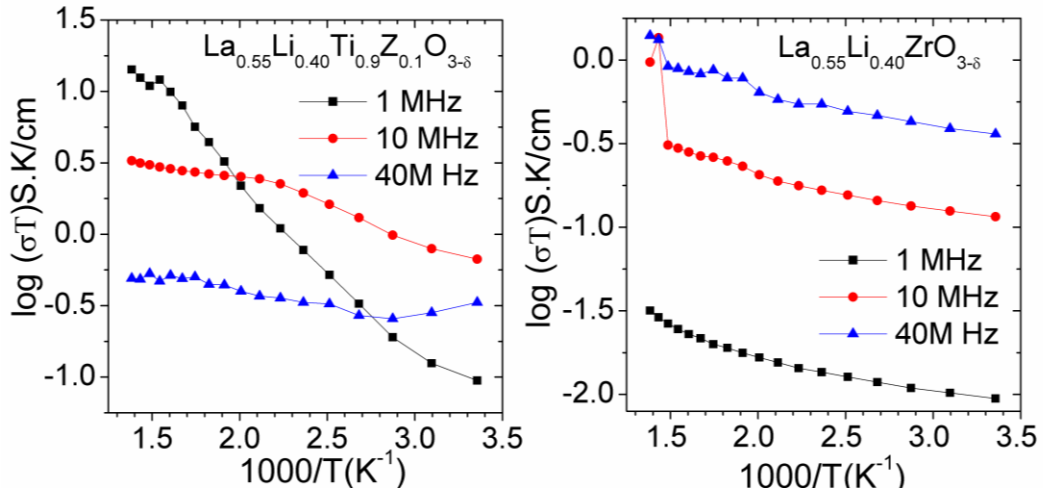


Fig. 4. Arrhenius plots for Li ion conductivity of $\text{La}_{0.55}\text{Li}_{0.40}\text{Ti}_{0.9}\text{Zr}_{0.1}\text{O}_{3-\delta}$ and $\text{La}_{0.55}\text{Li}_{0.40}\text{ZrO}_{3-\delta}$ at 1 MHz, 10MHz and 40MHz frequencies in ambient atmosphere in temperature range 25 to 450°C. The plotted conductivity represents the sum of the grain boundary and bulk conductivity.

Table1: Maximum AC conductivity (σ_{max} S/cm) value on the given frequency value obtained at tabulated temperatures

Samples	Maximum Conductivity (σ_{max} S/cm)			
	25°C	100°C	200°C	300°C
$\text{La}_{0.55}\text{Li}_{0.40}\text{TiO}_{3-\delta}$	2.61×10^{-3} at ~13MHz	4.13×10^{-3} at ~4MHz	1.58×10^{-2} at ~2.6MHz	3.20×10^{-2} at ~1MHz
$\text{La}_{0.55}\text{Li}_{0.40}\text{Ti}_{0.9}\text{Zr}_{0.1}\text{O}_{3-\delta}$	7.21×10^{-3} at ~17MHz	4.69×10^{-3} at 13MHz	6.23×10^{-3} at 6.7MHz	1.34×10^{-2} at 2.1MHz
$\text{La}_{0.55}\text{Li}_{0.40}\text{ZrO}_{3-\delta}$	1.02×10^{-2} at 30MHz	1.15×10^{-2} at 30MHz	1.90×10^{-2} at ~31MHz	5.21×10^{-2} at ~31MHz

Arrhenius plots for Li ion conductivity of $\text{La}_{0.55}\text{Li}_{0.40}\text{Ti}_{0.9}\text{Zr}_{0.1}\text{O}_{3-\delta}$ and $\text{La}_{0.55}\text{Li}_{0.40}\text{ZrO}_{3-\delta}$ at 1 MHz, 10MHz and 40MHz frequencies in ambient atmosphere in the temperature range 25°C to 450°C has been shown in figure 4.

$\text{La}_{0.55}\text{Li}_{0.40}\text{Ti}_{0.9}\text{Zr}_{0.1}\text{O}_{3-\delta}$ sample shows the increase in conductivity as temperature was increased from 25 to 450°C. The conductivity recorded at 1MHz shows steep increase in comparison to the conductivities recorded at 10 MHz and 40 MHz frequencies. $\text{La}_{0.55}\text{Li}_{0.40}\text{ZrO}_{3-\delta}$ sample shows the increase in conductivity from 25°C to 400°C at all three frequencies 1 MHz, 10 MHz and 40MHz. At temperatures greater than 400°C, conductivity value has been increased at frequencies 10 MHz and 40MHz for $\text{La}_{0.55}\text{Li}_{0.40}\text{ZrO}_{3-\delta}$. These changes in conductivity values show the change in ionic conductivity mechanism at higher temperatures.

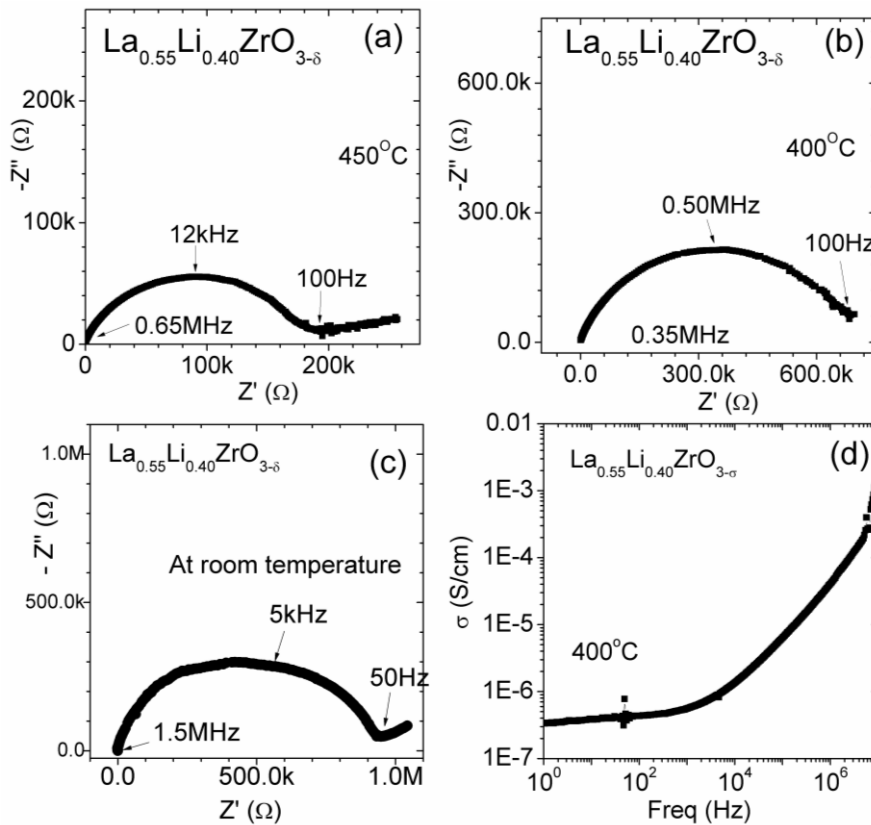


Fig. 5. (a), (b) and (c) show AC impedance plots of $\text{La}_{0.55}\text{Li}_{0.40}\text{ZrO}_{3-\delta}$ at 450, 400°C and RT(25°C). Figure 5 (d) shows AC conductivity vs frequency plots of $\text{La}_{0.55}\text{Li}_{0.40}\text{ZrO}_{3-\delta}$ at 400°C.

Figure 5 (a), (b) and (c) show the AC impedance plots (Cole - Cole) for $\text{La}_{0.55}\text{Li}_{0.40}\text{ZrO}_{3-\delta}$ at 450°C, 400°C and 25°C. Figure 5(d) shows the conductivity behaviour of $\text{La}_{0.55}\text{Li}_{0.40}\text{ZrO}_{3-\delta}$ sample at 400°C. Conductivity value has been found increasing with the frequency up to ~20MHz at 400°C. Increase in conductivity at higher temperatures indicates that the sample is thermally activated and ions jump into neighbouring vacant sites [27-28]. The Cole Cole plots show a single semicircle like behavior of $\text{La}_{0.55}\text{Li}_{0.40}\text{ZrO}_{3-\delta}$ from room temperature to 450°C. All the semicircles in Figs. 5 -a, b,c) merge and terminate on the real impedance axis at higher frequency side. This indicates the presence of only bulk resistance for these samples, and the grain boundary resistances are negligibly small as no second semicircle is observed. The behaviour of Cole-Cole plots show the ionic conduction occurs in $\text{La}_{0.55}\text{Li}_{0.40}\text{ZrO}_{3-\delta}$ through bulk of the sample.

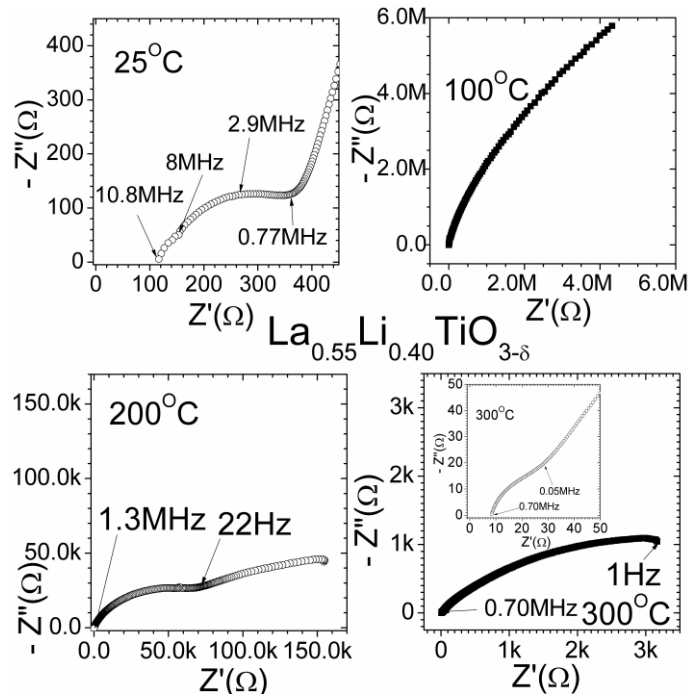


Fig. 6. AC impedance plots of $\text{La}_{0.55}\text{Li}_{0.40}\text{TiO}_{3-\delta}$ at 25°C, 100°C, 200°C and 300°C

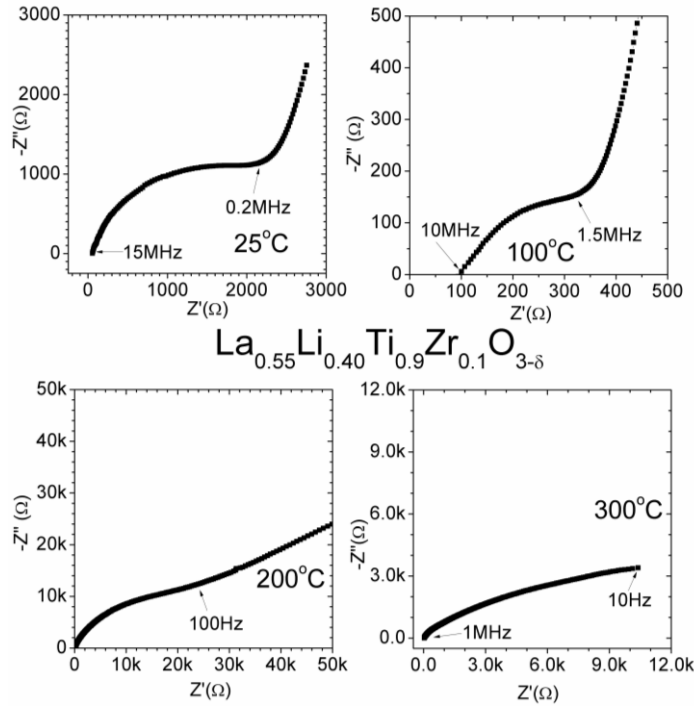


Fig. 7. AC impedance plots of $\text{La}_{0.55}\text{Li}_{0.40}\text{Ti}_{0.9}\text{Zr}_{0.1}\text{O}_{3-\delta}$ at 25°C , 100°C , 200°C and 300°C

Figure 6 and 7 show the AC impedance plots (Cole - Cole) for $\text{La}_{0.55}\text{Li}_{0.40}\text{TiO}_{3-\delta}$, $\text{La}_{0.55}\text{Li}_{0.40}\text{Ti}_{0.9}\text{Zr}_{0.1}\text{O}_{3-\delta}$ at 25°C , 100°C , 200°C and 300°C . Cole Cole plots show the typical ionic behaviour of $\text{La}_{0.55}\text{Li}_{0.40}\text{TiO}_{3-\delta}$, $\text{La}_{0.55}\text{Li}_{0.40}\text{Ti}_{0.9}\text{Zr}_{0.1}\text{O}_{3-\delta}$ at 25°C , 100°C , 200°C and 300°C . Li ion conduct in samples from room temperature to higher temperatures.

4. Conclusion

In conclusion, this is the first report where we have successfully synthesized $\text{La}_{0.55}\text{Li}_{0.40}\text{ZrO}_{3-\delta}$ and Zr doped $\text{La}_{0.55}\text{Li}_{0.40}\text{Ti}_{0.9}\text{Zr}_{0.1}\text{O}_{3-\delta}$ which crystallizes in orthorhombic crystal systems. Conductivities have been found increased at higher frequencies in $\text{La}_{0.55}\text{Li}_{0.40}\text{ZrO}_{3-\delta}$ and $\text{La}_{0.55}\text{Li}_{0.40}\text{Ti}_{0.9}\text{Zr}_{0.1}\text{O}_{3-\delta}$ in comparison to the conductivities of

La_{0.55}Li_{0.40}TiO_{3-δ} . Sintered pellet of La_{0.55}Li_{0.40}ZrO_{3-δ} shows very high conductivity 1.04 x 10⁻² S/cm at room temperature and up to 5.1 x 10⁻² S/cm conductivity at higher temperatures.

Acknowledgements

B. Singh thanks Dr. Mukul Gupta, UGC-DAE CSR, Indore Centre, India for his help in XRD data collection and UGC-DAE CSR, Indore Centre, India for financial support for CSR programme.

References

- [1] S Stramare , V Thangadurai and W Weppner, *Chem. Mater.* **15**, 3974(2003)
- [2] I Kokal, M Somer, P H L Notten and H T Hintzen, *Solid State Ionics* **185**, 42 (2011)
- [3] J B Goodenough, H Y-P Hong and J A Kafalas, *Mater. Res. Bull.* **11**, 203 (1976)
- [4] N Kamaya *et al. Nat. Mater.*, **10**, 682 (2011)
- [5] L Latie, G Villeneuve, D Conte and G L Flem J. *Solid State Chem.* **51**, 293 (1984)
- [6] A G Belous, G N Novitsukaya, S V Polyanetsukaya, Y I Gornikov and Izv Akad Russ. J. *Inorg. Chem* **32**, 1956 (1987)
- [7] B Singh *Phys. Chem. Chem. Phys.* **18**, 12947,(2016)
- [8] B Singh, R K Sahu, S S Manoharan, K. Dörr and K H Müller *J. Mag. Mater.* **273**, (2004) 358
- [9] V Thangadurai and W Weppner *J. Electrochem Soc.* **148**, A1294 (2001)
- [10] L Sebastian and J Gopalakrishnan *J. Mater. Chem.* **13**, 433 (2003)
- [11] B Singh *RSC Advances* **5**, 39938 (2015)
- [12] M V V Reddy, S S Manoharan, J John, B Singh, G V S Rao and M V R Chaudari *J. Electrochem. Soc.*, **156**, A652 (2009)
- [13] Y Harada, Y Hirakoso, H Kawai, J Kuwano, *Solid State Ionics* **121**, 245 (1999)
- [14] J A Alonso, J Sanz, J Santamaría, C León, A Várez, M T Fernández-Díaz, *Angew.Chem Int. Ed.* **39**, 619 (2000)

- [15] Y Inaguma, C Ligan, M Itoh, T Nakamura, T Uchida, H Ikuto, M Wakihara, *Solid Stat. Comm.* **86**, 689 (1993)
- [16] J Sanz, J A Alonso, A Varez, M T Fernández-Díaz, *J. Chem. Soc., Dalton Trans.* **7**, 1406 (2002).
- [17] Y Inaguma, T Katsumata, M Itoh, Y Morii, *J. Solid State Chem.* **166**, 67 (2002)
- [18] Y Harada, Y Hirakoso, H Kawai and J Kuwano *Solid State Ionics* **121**, 245 (1999).
- [19] C Uhlmann, P Braun, J Illig, A Weber, E Ivers-Tiffée *Journal of Power Sources* **307**, 578 (2016)
- [20] T T L Hang, T N Duc, J K Young, N P Choong and J P Chan, *Electrochimica Acta* **248**, 232 (2017)
- [21] N S P Bhuvanesh and J Gopalakrishnan *J. Mater. Chem.* **7**, 2297 (1997)
- [22] R Murugan , V Thangadurai and W Wepper *Angew. Chem. Int. Ed.* **46**, 7778 (2007)
- [23] S Ohta, T Kobayashi and T Asaoka, *J. Power Sources* **196**, 3342 (2011)
- [24] M Kotobuku, Y Suzuki, H Munakata, K Kanamura, Y Sato, K Yamamoto and T Yoshida *J. Electrochem. Soc.* **157**, A493 (2010).
- [25] H Jean, K V G Kutty and T R N Kutty *J Mater Sci* **40**, 4737 (2005).
- [26] A Belous, G Novitskaya, L Gavrilova, S Polyanetskaya and Z Makarova *Sov. Prog. Chem.* **51**, 13 (1985).
- [27] J R Donald *Impedance Spectroscopy* (Wiley, USA1987)
- [28] J L Souquet, M Levy and M Duclot *Solid State Ionics* **70**, 337 (1994)